Incorporating the effect of curvature on the sizing of spiral heat exchangers

M. Picón-Núñez[1,*], C. O. Ríos-Orozco[2], and J. M. Riesco-Ávila[2]

[1]Department of Chemical Engineering, University of Guanajuato, Noria Alta, S/N, Guanajuato, Gto., CP. 36050, [2]Department of Mechanical Engineering, University of Guanajuato, Carretera Salamanca-Valle de Santiago km. 3.5 + 1.8 km. Comunidad de Palo Blanco, Salamanca, Gto., México

ABSTRACT

In this paper, the effect that the continuous curvature change of spiral heat exchangers has upon the size of these types of units is analyzed. For single phase and laminar flow applications, curvature, represented by the Dean number, strongly affects the heat transfer coefficient. In a spiral heat exchanger, curvature changes take place at every position along the length of the channels through which the fluids flow; so, in order to assess the effect of curvature on the final design, the heat transfer coefficient needs to be continually updated and a finite element design approach implemented. This approach is compared to a design methodology reported in the literature that uses average heat transfer coefficients. Results show that for laminar flow applications, in the case of designs with both fluids having equal heat capacity flow rate –balanced exchangers-, the difference between using average heat transfer coefficients and locally updated values is less significant compared to the case of unbalanced applications.

KEYWORDS: spiral heat exchangers, design methodology, thermal effect of curvature, Dean number

NOMENCLATURE

A Heat transfer surface area (m^2)
A_c Free flow area (m^2)

*Corresponding author

b Plate spacing (m)
C Heat capacity mass flow rate ratio
C_C Cold fluid heat capacity mass flow rate (W/°C)
C_H Hot fluid heat capacity mass flow rate (W/°C)
C_p Heat capacity (J/kg °C)
D_h Hydraulic diameter (m)
D_s Spiral outer diameter (m)
d_s Spiral inner diameter (m)
f Friction factor
F_T Log mean temperature difference correction factor
h Heat transfer coefficient (W/m^2 °C)
H Plate width (m)
K Dean number
k Thermal conductivity (W/m °C)
L Plate length (m)
L_T Thermal length (m)
n Number of semi-turns
NTU Number of heat transfer units
Nu Nusselt number
$\dot{m}$ Mass flow rate (kg/s)
Pr Prandtl number
Q Heat load (W)
R Spiral curvature radius (m)
Re Reynolds number
R_o Inner most spiral radius (m)
R_{total} Thermal resistance (m^2 °C/W)
S Distance between hot and cold spirals (m)
T Hot fluid temperature (°C)
t Cold fluid temperature (°C)
ΔP Pressure drop (Pa)

ΔT_{lm} Log mean temperature difference (°C)
U Overall heat transfer coefficient (W/m^2 °C)

Greek symbols

α Friction factor related aspect ratio
γ Nusselt number related aspect ratio
δ Increment
ε_I Thermal effectiveness of a semi turn
μ Viscosity (kg/m s)
ρ Density (kg/m^3)
τ Plate thickness (m)
ϕ Angle of curvature

Subscripts

1   Plate side 1
2   Plate side 2
av   Average
C   Cold side
H   Hot side
I   Inlet
o   Outlet

INTRODUCTION

The geometrical features of spiral heat exchangers (SPHE) have an important effect upon its thermal performance. When a fluid moves in a direction going to the center of the unit, as shown in Figure 1, the continuous change in curvature results in an increased heat transfer coefficient, whereas a fluid moving in the outward direction will experience the opposite effect.
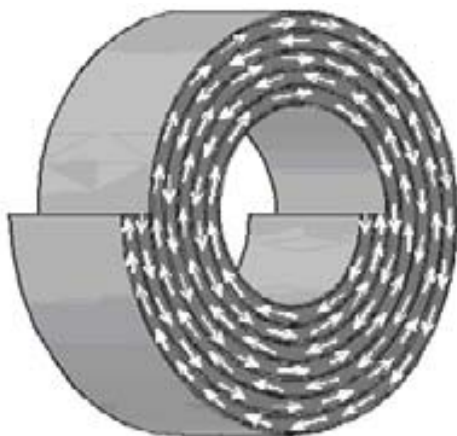

Figure 1. Flow arrangement inside a single phase spiral heat exchanger.

Most information available for the estimation of the heat transfer coefficients for this type of geometry is based on average values (Minton [1] and Martin [2]). Using this type of information, Picón-Núñez *et al.*, [3, 4] developed a simple methodology for the sizing of spiral heat exchangers. In their approach, the exchanger dimensions for which both streams fully absorb their specified pressure drop are determined. Next, these values are used to select the final exchanger geometry according to standard plate dimensions. This design approach uses empirical correlations for the prediction of the heat transfer and friction factor based on average curvature.

The effect of curvature upon the heat transfer coefficient is more pronounced in the laminar region than in the turbulent region. Egner and Burmeister [5] reported a numerical study based on computational fluid dynamics where the heat transfer process within a spiral duct with a rectangular cross section was analyzed; an expression for estimating the Nusselt number as a function of the Dean number was obtained. Their results demonstrate the great dependence of the heat transfer coefficient upon the curvature radius. They also showed that in the region of highest curvature (the center of the spiral), the heat transfer coefficient is 50% higher than the one found in the fully developed region of the same unit.

For the effect of curvature to be incorporated into a sizing methodology, an expression for the determination of local heat transfer coefficient is needed. Such an approach is implemented in this work; it consists in the definition of discrete elements of equal heat load where the heat transfer coefficient and the log mean temperature difference are calculated. The summation of the heat transfer area of each discrete element gives the overall exchanger surface area. Additionally, the comparison is made between the sizes of a SPHE using a finite element design approach as opposed to that obtained using an integral approach. The balanced or unbalanced characteristic of a SPHE is considered in this investigation (Burmeister [6]).

DESIGN METHODOLOGY

The design of a heat exchanger refers to the determination of the geometry that will transfer the required heat duty within the constraints of

pressure drop. In any design approach there are some dimensions that must be specified ahead of design. In the case of a SPHE, the geometry that must be specified includes: plate spacing between plates for each stream, the internal spiral diameter, the external diameter and the flow passage width (Picón *et al.*, [6]). A detailed description of the expressions for the determination of the spiral diameter, the plate length and number of turns given the complex geometrical features of a spiral heat exchanger have been presented by Dongwu [7]. The calculation of a SPHE proceeds in the following manner: the exchanger heat load is worked out from a simple heat balance as:

$$Q = C_C(t_0 - t_i) = C_H(T_i - T_0) \tag{1}$$

Once the exchanger heat load is known, the exchanger is divided into *n* elements of equal heat load Q_i and the corresponding element surface area is determined using the design equation:

$$A_i = \frac{Q_i}{U_i \, F_{T,i} \, \Delta T_{lm,i}} \qquad i = 0,1,2,.....n \tag{2}$$

Where the log mean temperature difference $\Delta T_{lm,i}$ is calculated from:

$$\Delta T_{ml,i} = \frac{(T_{H,i} - t_{C,i+1}) - (T_{H,i+1} - t_{C,i})}{\ln\left(\dfrac{T_{H,i} - t_{C,i+1}}{T_{H,i+1} - t_{C,i}}\right)} \qquad i = 0,1,2,.....n \tag{3}$$

The overall heat transfer coefficient (U_i) is determined from:

$$U_i = \frac{1}{R_{total,i}} \qquad i = 0,1,2,.....n \tag{4}$$

$$R_{total,i} = \frac{1}{h_{H,i}} + \frac{\tau}{k} + \frac{1}{h_{C,i}} \qquad i = 0,1,2,.....n \tag{5}$$

In the case of an average heat transfer coefficient, an expression for determining the Nusselt number is:

$$Nu = 0.04 \, \mathrm{Re}^{0.74} \, \mathrm{Pr}^{0.4} \tag{6}$$

Where the Nusselt number is defined as:

$$Nu = \frac{h D_h}{k} \tag{7}$$

For the case where the effect of curvature is considered, Egner and Burmeister [5] introduced

the following expressions that apply in the laminar region:

$$\frac{Nu_i}{Nu_o} = 1 + 0.0429\left(\frac{K_{av,i}}{\gamma}\right)^{0.68} \mathrm{Pr}^{0.4} \qquad i = 0,1,2,.....n \tag{8}$$

This expression applies for the following conditions: $1 \le \gamma \le 4$; $0 \le K_{av,i} \le 364$; $0.7 \le \mathrm{Pr} \le 5$. Whereas for the following conditions: $1 \le \gamma \le 8$; $0 \le K_{av,i} \le 384$; $0.7 \le \mathrm{Pr} \le 5$, the equation that applies is:

$$\frac{Nu_i}{Nu_o} = 1 + 0.0767\left(\frac{K_{av,i}}{\gamma}\right)^{0.57} \mathrm{Pr}^{0.4} \qquad i = 0,1,2,.....n \tag{9}$$

The values of Nu_0 are the following: $Nu_0 = 4.08$ for $\gamma = 1$; $Nu_0 = 5.64$ for $\gamma = 4$ and $Nu_0 = 6.01$ for $\gamma = 8$. The aspect ratio γ, is given by:

$$\gamma = \frac{H}{b} \tag{10}$$

The local average Dean number is defined as:

$$K_{av,i} = \frac{K_{1,i} + K_{2,i}}{2} \qquad i = 0,1,2,.....n \tag{11}$$

$$K_{1,i} = \mathrm{Re}\left[\frac{D_h}{R_{1,i}}\right]^{1/2} \qquad i = 0,1,2,.....n \tag{12}$$

$$K_{2,i} = \mathrm{Re}\left[\frac{D_h}{R_{2,i}}\right]^{1/2} \qquad i = 0,1,2,.....n \tag{13}$$

For an Archimedean spiral we have that:

$$R_{1,i} = \frac{s\phi_i}{\pi} + R_{01} \qquad i = 0,1,2,.....n \tag{14}$$

$$R_{2,i} = \frac{s\phi_i}{\pi} + R_{02} \qquad i = 0,1,2,.....n \tag{15}$$

Despite the fact that in a spiral heat exchanger the relative flow of fluids is countercurrent, the temperature field distortions originated within the unit, require a temperature correction factor to be applied. Martin [2], developed an expression for the determination of the correction factor of the log mean temperature difference. The expression is:

$$F_{T,i} = \frac{1}{(1+C)NTU_i/n_i}\ln\left(1 + \frac{1+C}{(1/\varepsilon_{i,i})-1}\right) \qquad i = 0,1,2,.....n \tag{16}$$

Where NTU is the number of heat transfer units, ε_i is the thermal effectiveness per turn and *n* is the

number of semi-turns. The two former terms are respectively given by:

$$NTU_i = \frac{U_i A_i}{(\dot{m}Cp)_{min}} \qquad i = 0,1,2,.....n \qquad (17)$$

$$\varepsilon_{i,i} = \frac{1-e^{-(1+C)NTU_i/n_i}}{1+C} \qquad i = 0,1,2,.....n \qquad (18)$$

Dongwu [7] provides the expression for the determination of the number of semi-turns (*n*) and the spiral external diameter:

$$n_i = \frac{-(d_s - \tau/2) + \sqrt{(d_s - \tau/2)^2 + 4\tau L_i/\pi}}{\tau} \qquad i = 0,1,2,.....n \quad (19)$$

$$D_{s,i} = \sqrt{1.28\tau_1 L_i + d_s^2} \qquad i = 0,1,2,.....n \qquad (20)$$

Where τ_1 is defined as:

$$\tau_1 = (b_H + b_C) + 2\tau \qquad (21)$$

The length of each discrete element A_i can be calculated from:

$$A_i = H(L_{1i} + L_{2i}) \qquad i = 0,1,2,.....n \qquad (22)$$

In order to determine the spiral radius (*R*), the angle of curvature (ϕ) has to be calculated. To this end, an iterative approach is implemented. The value of the length of each discrete element ($L_{1i,}$ and L_{2i}) that corresponds to the arch length projected by the angle ϕ_i (see Figure 2) is given by:

$$L_i = \int_0^{\phi_i} \left(\sqrt{\left(\frac{dR_i}{d\phi}\right)^2 + R_i^2} \right) d\phi \qquad i = 0,1,2,.....n \qquad (23)$$

After integration of the equation above we have:

$$L_i = \frac{\pi}{2s} \left[\left(\frac{s\phi_i}{\pi} + R_o\right)\sqrt{\left(\frac{s}{\pi}\right)^2 + \left(\frac{s\phi_i}{\pi} + R_o\right)^2} - R_o\sqrt{\left(\frac{s}{\pi}\right)^2 + R_o^2} + \left(\frac{s}{\pi}\right)^2 \ln\left(\frac{\left(\frac{s\phi_i}{\pi} + R_o\right) + \sqrt{\left(\frac{s}{\pi}\right)^2 + \left(\frac{s\phi_i}{\pi} + R_o\right)^2}}{\left(R_o + \sqrt{\left(\frac{s}{\pi}\right)^2 + R_o^2}\right)} \right) \right] \qquad (24)$$

The following parameters are calculated for each stream:

Reynolds number:

$$Re = \frac{D_h \dot{m}}{\mu A_C} \qquad (25)$$

Hydraulic diameter:

$$D_h = \frac{2bH}{b+H} \qquad (26)$$

Free flow area:

$$A_C = bH \qquad (27)$$

Prandtl number:

$$Pr = \frac{Cp\mu}{k} \qquad (28)$$

Heat capacity mass flow rate ratio:

$$C = \frac{(\dot{m}Cp)_{min}}{(\dot{m}Cp)_{max}} \qquad (29)$$

The pressure drop through the exchanger core can be calculated from:

$$\Delta P_i = \frac{2f L_i \dot{m}^2}{\rho D_h A_C^2} \qquad i = 0,1,2,.....n \qquad (30)$$

Where *f* is the friction factor that for the laminar, transition and turbulent flow can respectively be calculated from the following equations (Hesselgreaves [8]):

$$f\,Re = 24\big(1 - 1.3553\alpha + 1.9467\alpha^2 - 1.7012\alpha^3 \\ + 0.9564\alpha^4 - 0.2537\alpha^5\big) \qquad (31)$$

$$f = 0.0054 + \frac{2.3x10^{-8}}{Re^{-3/2}} \qquad (32)$$

$$\frac{1}{\sqrt{f}} = 1.56\ln(Re) - 3.00 \qquad (33)$$

Where the parameter α is defined as:
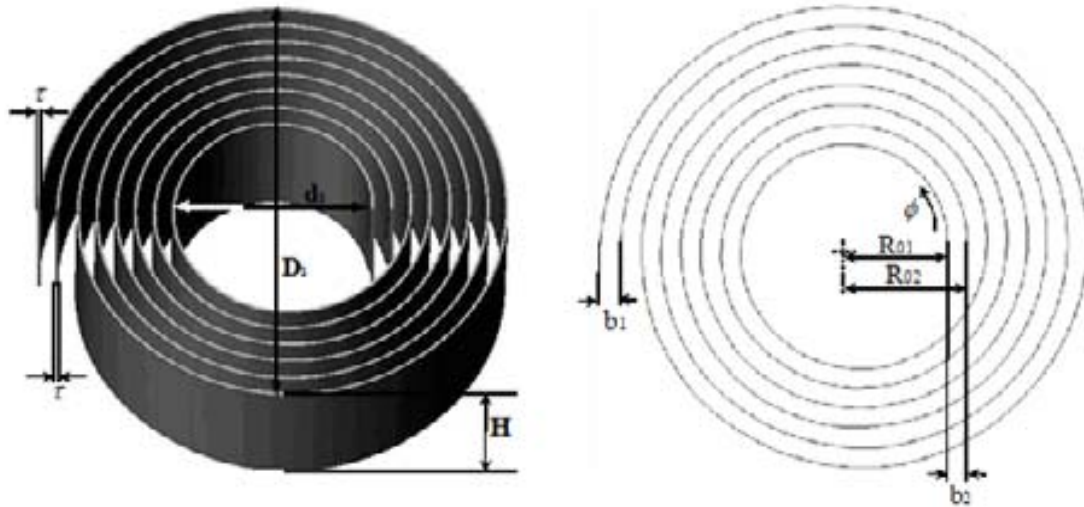
$$\alpha = \frac{b}{H} \qquad (34)$$

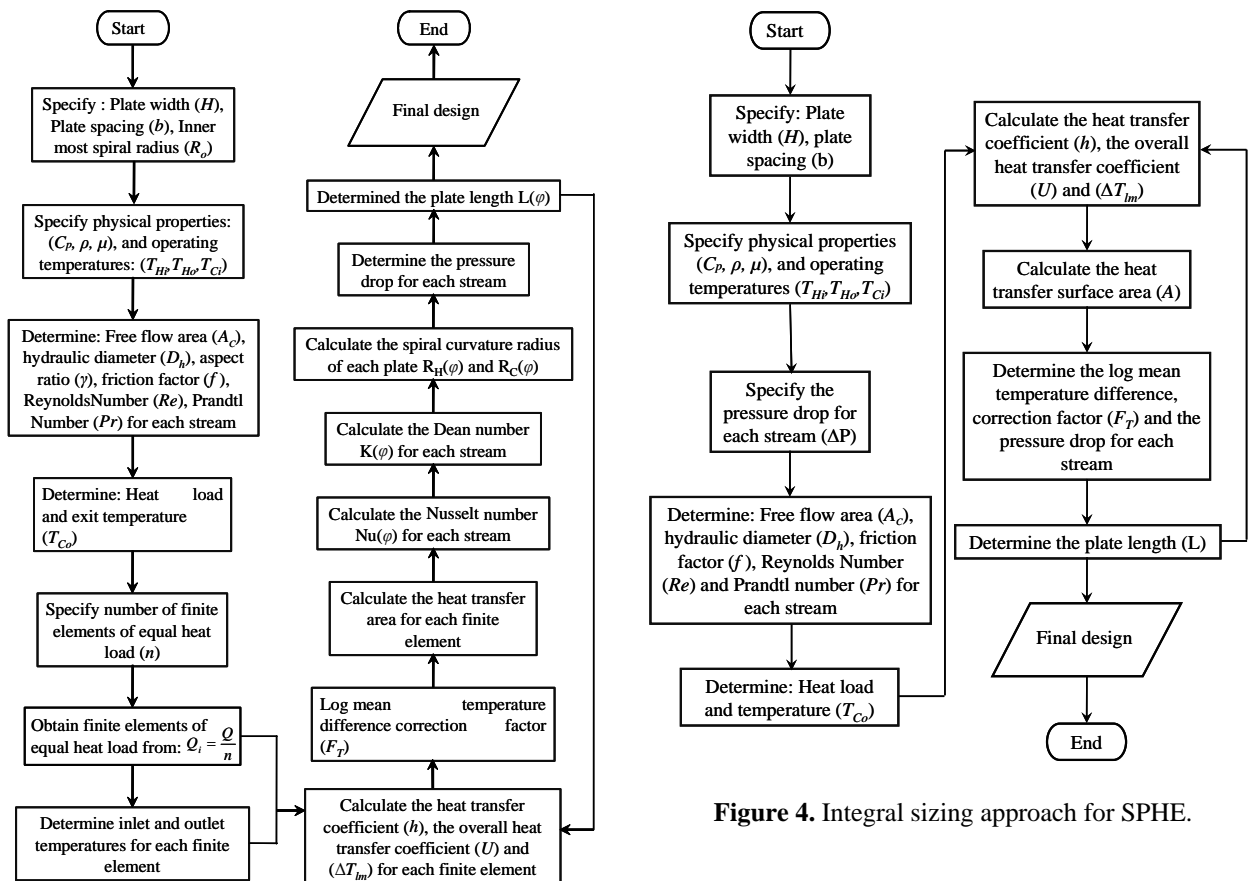**Figure 2.** Basic geometrical features of a spiral heat exchanger.

Figure 3. Discrete element sizing approach for SPHE. Heat transfer coefficients locally updated to consider the effect of curvature.

Figure 4. Integral sizing approach for SPHE.

The flow diagram of the discrete element sizing approach and the integral methodology (Picón-Núñez *et al.* [4]) are respectively shown in Figures 3 and 4.

CASE STUDIES

Four case studies are analyzed in this section. The operating data, physical properties and geometrical information are given in Tables 1 and 2. In the case of Table 1, case studies 1 and 2 correspond to balanced exchanger applications ($C_H = C_C$) whereas case studies 3 and 4 in Table 2, correspond to unbalanced design problems ($C_H \neq C_C$). The application of the design approach is described in the following section.

RESULTS

Tables 3 and 4 show the design results obtained using the two methodologies for cases 1 and 2. For the purposes of comparison, the discrete element sizing approach is solved for two cases: one where the heat transfer coefficient is locally updated and other where the heat transfer coefficient is assumed constant. In the case of balanced heat exchangers when constant heat transfer coefficients are assumed, the results using both methodologies are identical. However, when the effect of curvature is incorporated and the heat transfer coefficients are updated, the resulting surface area reduces by 18.5% in case 1 and 25% in case 2 compared to the case where the design is carried out using an integral approach and constant heat transfer coefficients.

The case of unbalanced heat exchangers, cases 3 and 4, are presented in Tables 5 and 6. In both cases, the finite element approach that incorporates the effect of curvature gives the smallest heat transfer area. Even using the constant heat transfer coefficients assumption, the discrete element approach still results in smaller units compared to the integral method. In case study 3, the design using discrete elements and updated heat transfer coefficients is 26.1% smaller compared to the integral design approach that use average values. In case study 4, the difference is as big as 53.9%. One reason that explains this is that the log mean temperature difference has a constant value throughout the unit in the case of the integral approach, whereas in the case of the discrete element approach, the local log mean temperature difference varies and overall it shows a larger mean value.

Table 1. Operating data, physical properties and geometrical information for case studies 1 and 2.

	Case study 1		Case study 2	
	Hot stream	Cold stream	Hot stream	Cold stream
Mass flow rate (kg/s)	0.1051	0.1131	0.1125	0.0609
Inlet temperature (°C)	200	60	130	20
Outlet temperature (°C)	120	140	85	65
Heat capacity (J/kg °C)	2973	2763	2264	4183
Thermal conductivity (W/m °C)	0.348	0.322	0.1357	0.5861
Density (kg/m^3)	843	843	834.3	994
Viscosity (kg/m s)	3.35×10^{-3}	8.0×10^{-3}	1.312×10^{-2}	1.002×10^{-3}
Plate thickness (m)	3.175×10^{-3}			
Thermal conductivity of material of construction (W/m°C)	17.3			
Plate spacing (m)	0.02			
Inner spiral radius (m)	0.09			

Table 2. Operating data, physical properties and geometrical information for case studies 3 and 4.

	Case study 3		Case study 4	
	Hot stream	Cold stream	Hot stream	Cold stream
Mass flow rate (kg/s)	0.0507	0.0605	0.0294	0.0453
Inlet temperature (°C)	130	10	90	20
Outlet temperature (°C)	90	40.17	30	58.91
Heat capacity (J/kg °C)	3076	3415	4183	4183
Thermal conductivity (W/m°C)	0.136	0.252	0.641	0.6107
Density (kg/m^3)	836	1104.4	983.2	994
Viscosity (kg/m s)	1.41×10^{-3}	1.57×10^{-3}	4.666×10^{-4}	7.196×10^{-4}
Plate thickness (m)	3.175×10^{-3}			
Thermal conductivity of material of construction (W/m°C)	17.3			
Plate spacing (m)	0.025		0.02	
Inner spiral radius (m)	0.09			

Table 3. Design results for case study 1.

	Finite element approach		Integral approach
	Curvature effect	Constant heat transfer coefficient	Constant heat transfer coefficient
Heat transfer surface area (m^2)	7.32	8.96	8.96
Re (Hot fluid)	348.6	348.6	348.6
Re (Cold fluid)	157.1	157.1	157.1
Heat duty (W)	25,000	25,000	25,000
Hot side heat transfer coefficient (W/m^2·°C)	169.6 - 126.9	113.96	113.96
Cold side heat transfer coefficient (W/m^2·°C)	142 - 110.6	82.95	82.95
Overall heat transfer coefficient (W/m^2·°C)	76.2 - 58.5	47.6	47.6
Plate width (m)	0.16	0.16	0.16
Plate length 1 (m)	22.2	27.2	27.98
Plate length 2 (m)	23.6	28.8	27.98
Inner spiral diameter (m)	0.203	0.203	0.203
Pressure drop hot side (Pa)	94.5	115.8	119.13
Pressure drop cold side (Pa)	258.1	314.9	306.1
Outer spiral diameter (m)	1.2	1.32	1.30

Table 4. Design results for case study 2.

	Finite element approach		Integral approach
	Curvature effect	Constant heat transfer coefficient	Constant heat transfer coefficient
Heat transfer surface area (m^2)	4.28	5.7	5.7
Re (Hot fluid)	95.3	95.3	95.3
Re (Cold fluid)	675.4	675.4	675.4
Heat duty (W)	11,464.6	11,464.6	11,464.6
Hot side heat transfer coefficient (W/m^2·°C)	69.46 - 53.7	38.40	38.40
Cold side heat transfer coefficient (W/m^2·°C)	247.2 - 201	179.8	179.8
Overall heat transfer coefficient (W/m^2·°C)	53.7 - 42.1	31.5	31.5
Plate width (m)	0.16	0.16	0.16
Plate length 1 (m)	12.88	17.2	17.81
Plate length 2 (m)	13.9	18.4	17.81
Inner spiral diameter (m)	0.203	0.203	0.203
Pressure drop hot side (Pa)	232.4	310.4	321.34
Pressure drop cold side (Pa)	8.7	11.5	11.15
Outer spiral diameter (m)	0.93	1.07	1.05

Table 5. Design results for case study 3.

	Finite element approach		Integral approach
	Curvature effect	Constant heat transfer coefficient	Constant heat transfer coefficient
Heat transfer surface area (m^2)	2.54	3.25	3.44
Re (Hot fluid)	319.4	319.4	319.4
Re (Cold fluid)	342.5	342.5	342.5
Heat duty (W)	6233.2	6233.2	6,233.2
Hot side heat transfer coefficient (W/m^2·°C)	54.82 - 44.33	34.87	34.87
Cold side heat transfer coefficient (W/m^2·°C)	90.17 - 75.75	57.87	57.87
Overall heat transfer coefficient (W/m^2·°C)	33.9 - 27.9	21.7	21.7
Plate width (m)	0.2	0.2	0.2
Plate length 1 (m)	5.99	7.7	8.61
Plate length 2 (m)	6.72	8.56	8.61
Inner spiral diameter (m)	0.203	0.203	0.203
Pressure drop hot side (Pa)	2.14	2.75	3.07
Pressure drop cold side (Pa)	2.41	3.07	3.09
Outer spiral diameter (m)	0.72	0.81	0.81

Table 6. Design results for case study 4.

	Finite element approach		Integral approach
	Curvature effect	Constant heat transfer coefficient	Constant heat transfer coefficient
Heat transfer surface area (m^2)	2.57	3.28	5.51
Re (Hot fluid)	700	700	700
Re (Cold fluid)	700	700	700
Heat duty (W)	7,378	7,378	7,378
Hot side heat transfer coefficient (W/m^2·°C)	232.2 - 196.3	143.5	143.5
Cold side heat transfer coefficient (W/m^2·°C)	238.9 - 203.1	165.75	165.75
Overall heat transfer coefficient (W/m^2·°C)	115.3 - 98.02	75.84	75.84
Plate width (m)	0.16	0.16	0.16
Plate length 1 (m)	7.68	9.83	17.23
Plate length 2 (m)	8.42	10.69	17.23
Inner spiral diameter (m)	0.203	0.203	0.203
Pressure drop hot side (Pa)	1.09	1.39	2.45
Pressure drop cold side (Pa)	2.81	3.58	5.76
Outer spiral diameter (m)	0.73	0.82	1.03

Figure 5 shows the variation of the Nusselt number with the length for cases 1 and 2. The curves for the two scenarios are plotted; they correspond to the assumption of constant heat transfer coefficient (equation 6) and incorporation of the curvature effect (equation 8). The curves have been extrapolated in order to have a better picture of the tendency of the Nusselt number at longer flow lengths. The part of the exchanger that corresponds to the zero flow length is the core of the unit, this is, the entrance of the hot fluid and the exit of the cold fluid. In this region, the
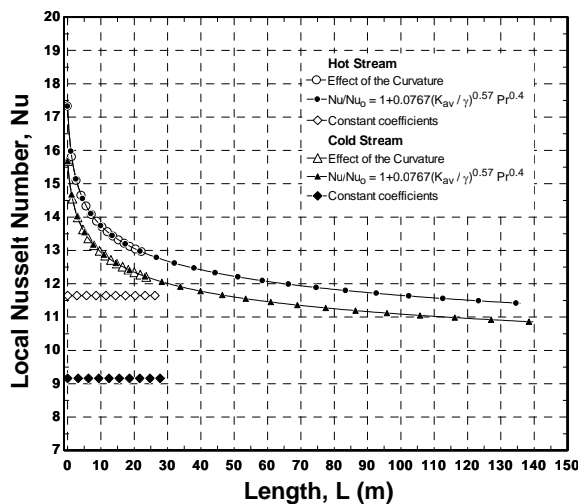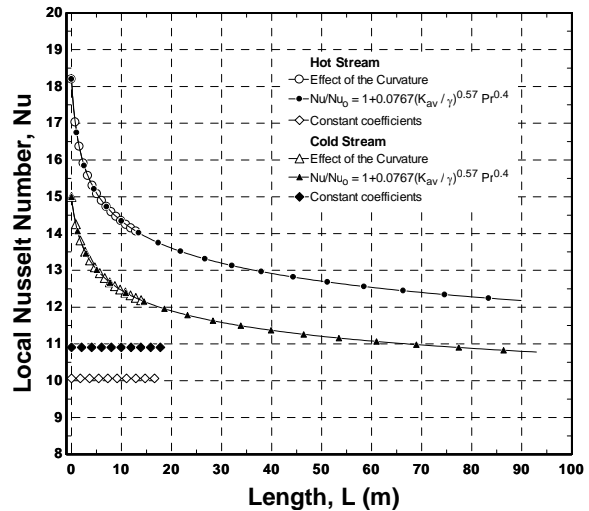
a) Case study 1   b) Case study 2

Figure 5. Variation of the Nusselt number with the flow length. Case studies 1 and 2.

heat transfer coefficients are higher than those in the outer most part of the exchanger and as the flow develops, the Nusselt number tends to reach an asymptotic value.
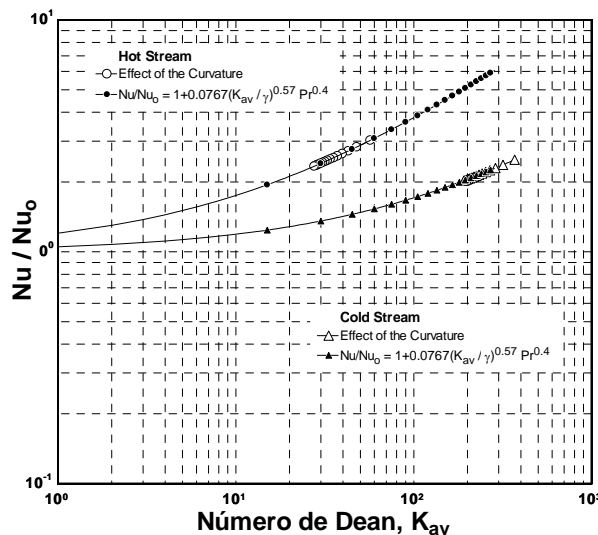
Figure 6 shows the variation of the Nusselt number as a function of the curvature represented by the Dean number. The higher the values of the Dean number the higher the curvature and consequently the higher the Nusselt number. Figure 7 shows the influence of the curvature radius on the Dean number.

Since curvature is inversely related to the curvature radius, then for a given Reynolds number, the Dean number increases as the curvature radius decreases.

The increase of pressure drop with the length for a given Reynolds number is presented in Figure 8. As expected, for a fixed free flow area, pressure drop varies linearly with the flow length and the slope of the curves is determined by the mass flow rate. For case studies 3 and 4 the results are shown in Figures 9, 10, 11 and 12.
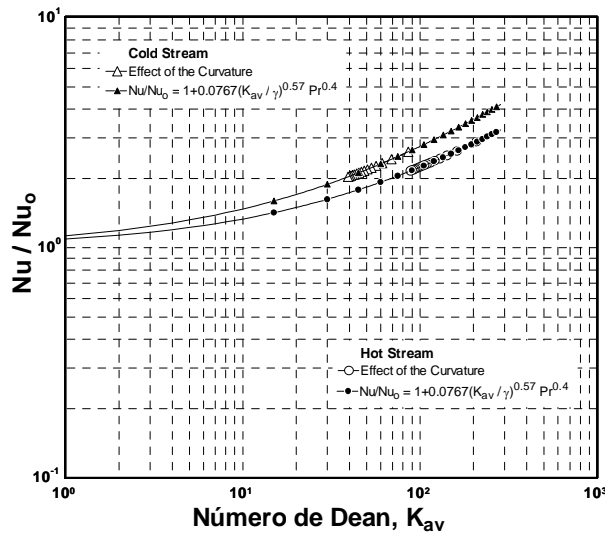
a) Case study 1

b) Case study 2

Figure 6. Variation of the Nusselt number with the Dean number. Case studies 1 and 2.
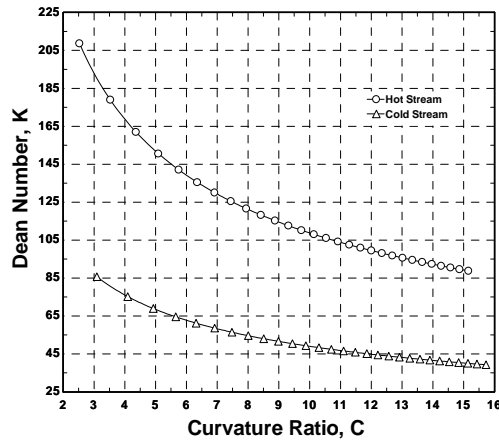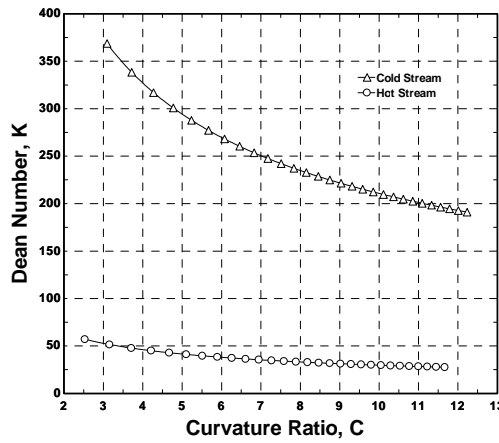
a) Case study 1

b) Case study 2

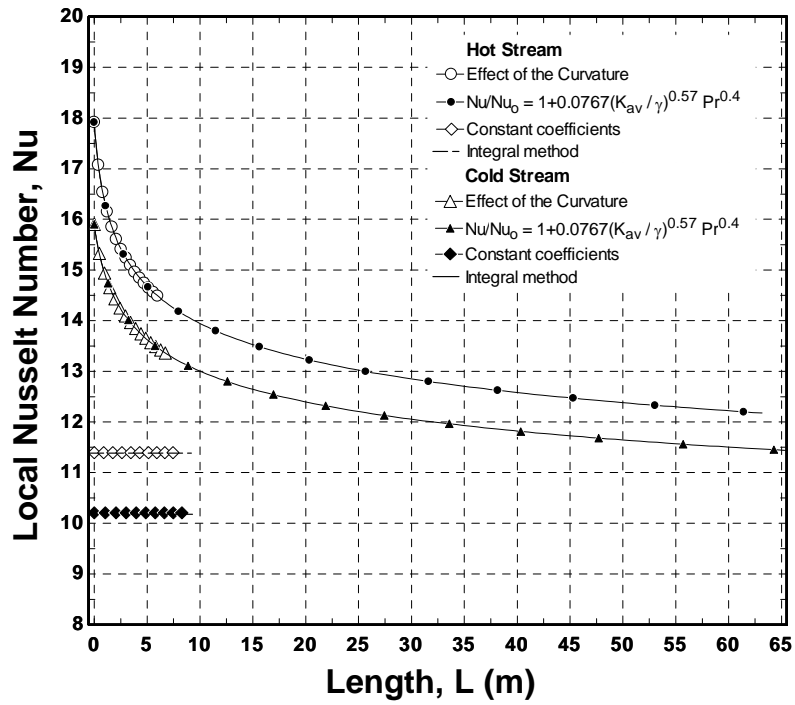**Figure 7.** Variation of the Dean number with curvature radius. Case studies 1 and 2.
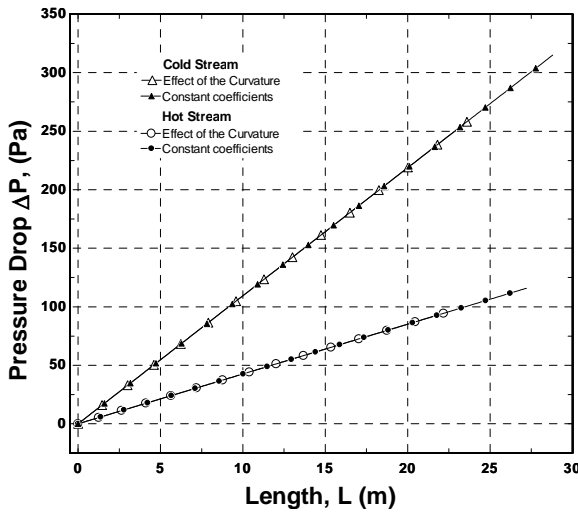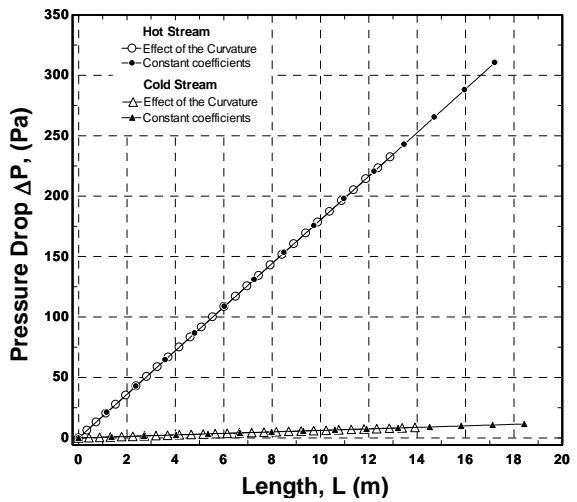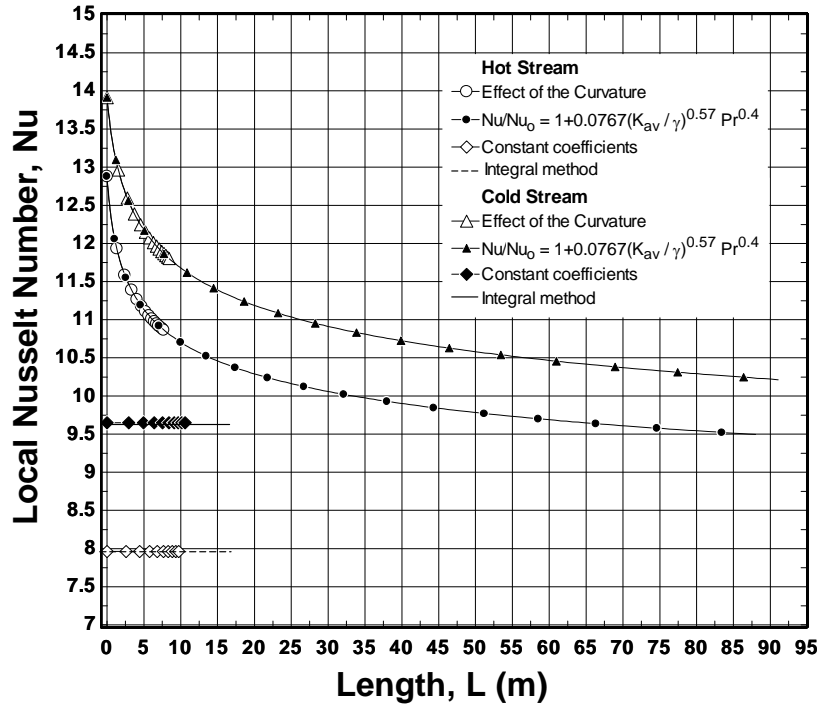

a) Case study 1

b) Case study 2

Figure 8. Variation of pressure drop with length for a given Reynolds number. Case studies 1 and 2.
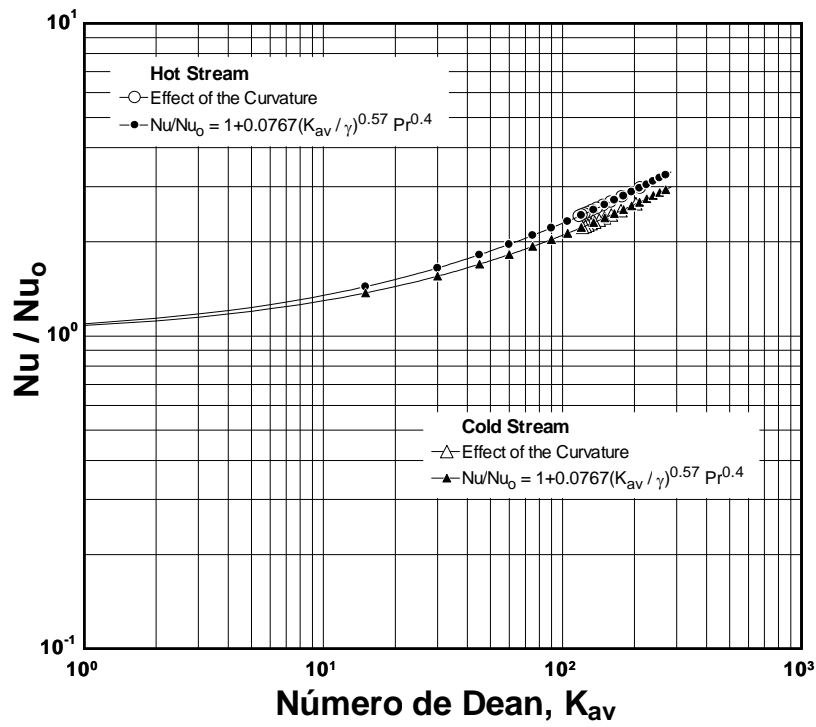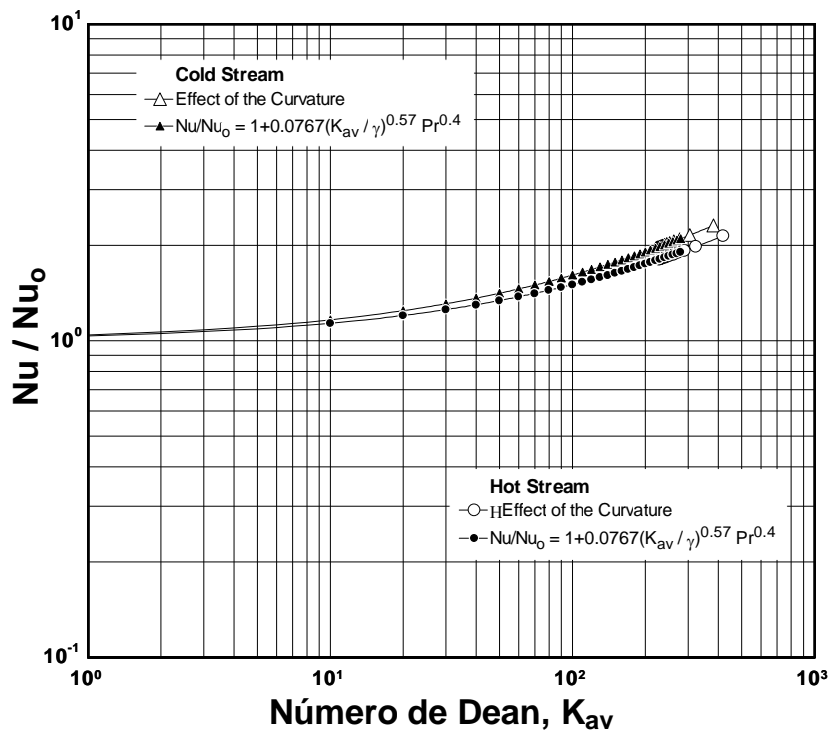
a) Case study 3

b) Case study 4

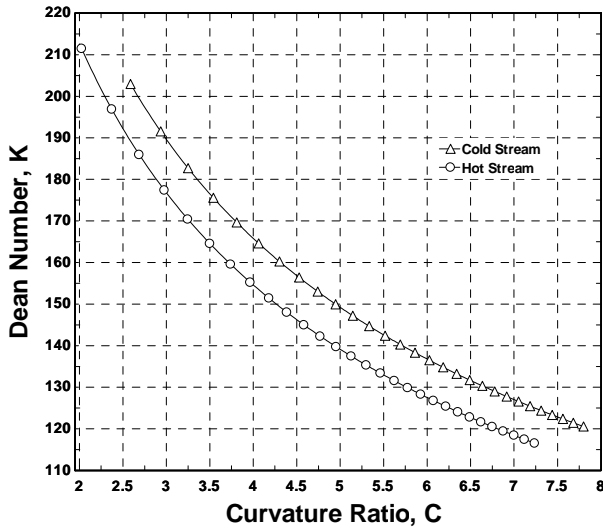**Figure 9.** Variation of the Nusselt number with the flow length. Case studies 3 and 4.
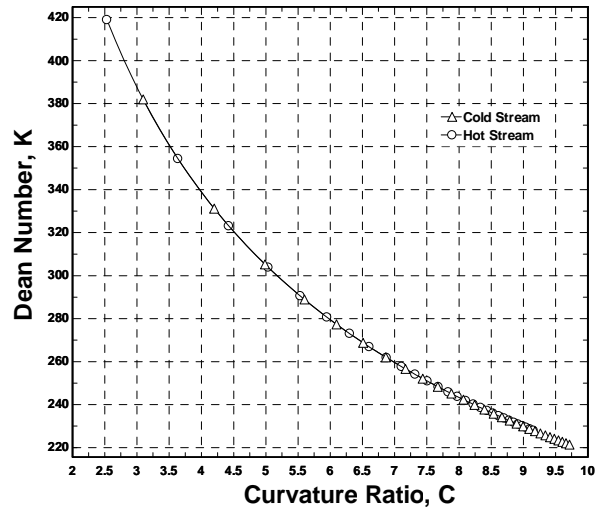
a) Case study 3

b) Case study 4

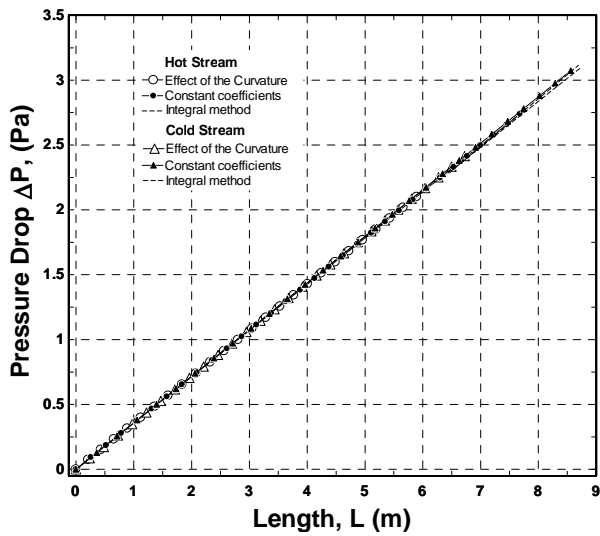**Figure 10.** Variation of the Nusselt number with the Dean number. Case studies 3 and 4.
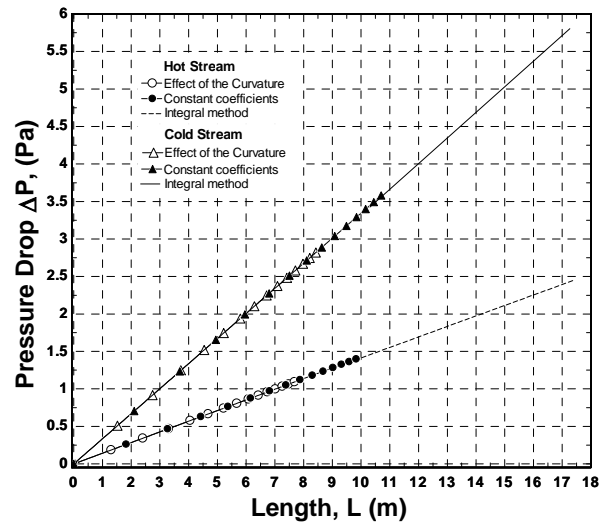
a) Case study 3

b) Case study 4

Figure 11. Variation of the Dean number with curvature radios. Case studies 3 and 4.

a) Case study 3

b) Case study 4

Figure 12. Variation of pressure drop with length for a given Reynolds number. Case studies 3 and 4.

CONCLUSIONS

The strong functionality of the heat transfer coefficient with respect to the curvature in spiral heat exchangers has an important effect upon the size of the unit. This functionality is more pronounced in the laminar region where the local heat transfer coefficients are higher than the ones obtained using expressions based on average curvature. When local heat transfer coefficients are used in design, the result is a heat exchanger with lower surface area compared to the size that would be obtained using average heat transfer coefficients. This study has shown that for the case of unbalanced exchangers, the level of overdesign is more significant

compared to the case of balanced applications. In the former case, two factors contribute to the increased effect on the size: one is the higher heat transfer coefficients and the other are the larger temperature driving forces that result as a finite element design methodology is implemented. The effect of curvature on the heat transfer coefficients reduces in the turbulent region; however, for the effect upon design to be assessed, expressions for the local heat transfer coefficient are still to be developed.

REFERENCES

1. Minton, P. E. 1970, Chemical Engineering, 103-112, May.
2. Martin, H. 1992, Heat Exchangers, Hemisphere Publishing Corporation.
3. Picón-Núñez, M., Canizalez-Dávalos, L., Martínez-Rodríguez, G., and Polley, G. T. 2007, Food and Bioproducts Processing, Trans IChemE, Part C, 85, C4, 322.
4. Picón-Núñez, M., Canizalez-Dávalos, L., and Medina Flores, M. 2009, Heat Transfer Engineering, 30, 9, 744.
5. Egner, M. W. and Burmeister, L. C. 2005, Journal of Heat Transfer, 127, 352.
6. Burmeister, L. C. 2006, Journal of Heat Transfer, 128, 295.
7. Dongwu, W. 2003, Chemical Engineering Technology, 26, 592.
8. Hesselgreaves, J. E. 2001, Compact heat exchangers, Pergamon Press.